PROPULSION KINETICS OF RECUMBENT HANDCYCLING DURING HIGH AND MODERATE INTENSITY EXERCISE

BY

KELLIE M. HALLORAN

THESIS

Submitted in partial fulfillment of the requirements
for the degree of Master of Science in Mechanical Engineering
in the Graduate College of the
University of Illinois Urbana-Champaign, 2022

Urbana, Illinois

Adviser:

Associate Professor Mariana Kersh

ABSTRACT

People with spinal cord injuries (PwSCI) are at high risk of developing cardiovascular disease (CVD). While regular exercise can reduce risk of CVD, PwSCI face various barrier to exercise, including high rates of upper limb soft tissue injuries, especially in the shoulder. Handcycling high intensity interval training (HIIT), which consists of periods of high intensity exercise followed by rest, is a potential exercise solution, but the musculoskeletal safety of HIIT is still unknown. In this study, we characterized three-dimensional continuous applied forces at the handle during handcycling HIIT and moderate intensity continuous training (MICT). These applied shoulder forces can give an early indication of joint loading, and therefore injury risk, at the shoulder. In all three directions (tangential, radial, and lateral), the maximum applied forces during HIIT were larger than those found in MICT at all timepoints, which may indicate higher contact forces and loads on the shoulder during HIIT compared to MICT. The tangential and radial forces peaked twice in a propulsion cycle, while the lateral forces peaked once. Throughout the exercise protocols, the location of tangential peak 2 and radial peak 1 was later in HIIT compared to MICT. This difference in maximum force location could indicate altered kinematics at the end of the exercise protocol. These changes in kinematics should be more closely examined using motion capture or other modeling techniques. If we combine this kinetic data with kinematic data during propulsion, we can begin to create musculoskeletal models that more accurately predict contact forces and injury risk during handcycling HIIT in PwSCI.

To my parents, who have been my biggest cheerleaders and most consistent sources of encouragement, help, and support.

ACKNOWLEDGMENTS

Thank you to Dr. Mariana Kersh for her support both in undergraduate and graduate school - you have allowed me to pursue a research project I'm interested in, ask questions, and make mistakes along the way. I would also like to thank the members of the Tissue Biomechanics Lab for their support and help along the way. Thank you specifically to Michael Focht, Griffin Sipes, Roberto Guzman, Alex Teague, and Michael Rogalski for their assistance with data collection and Ethan Park and Danielle Siegel (from the BABI lab, Boise State University) for their assistance with data labelling and processing.

Thank you to Dr. Joseph Peters and Dr. Ian Rice for their collaborative efforts in study design, participant recruitment, and data collection. I look forward to many more future collaborations and so appreciate your insight and opinions throughout this entire process. Thank you as well to Kathryn Huang, Kaushik Parkari, Kavin Lavari, and Isaac Soloveychik from the Wheelchair Biomechanics Laboratory for their assistance with data collection and labelling.

I could not have finished this project without the consistent support of my fellow graduate students and engineers. Thank you to Kayla Russell and Allisa Hastie for your friendship and encouragement in graduate school. Lastly, thank you to my undergraduate MechSE friends - I would not be here without your support and community through the late nights of homework, exams, and projects.

This project was funded in part by the National Science Foundation and the American Society of Biomechanics.

TABLE OF CONTENTS

CHAPTER 1 INTRODUCTION 1
1.1 Clinical Motivation 1
1.2 Handcycling 2
1.3 High Intensity Interval Training 4
1.4 Handcycling Kinetics and Reaction Forces 5

CHAPTER 2 LITERATURE REVIEW 8
2.1 Attach-Unit Handcycling 9
2.2 Recumbent Handcycling 10
2.3 Remaining Questions 13

CHAPTER 3 METHODS 16
3.1 Participants 16
3.2 Exercise Protocols 16
3.3 Handcrank Kinetics 18
3.4 Data Analysis 18
3.5 Statistical Analysis 19

CHAPTER 4 RESULTS 20
4.1 Participants 20
4.2 Maximum Force Magnitudes 20
4.3 Maximum Force Locations 23

CHAPTER 5 DISCUSSION 26
5.1 Maximum Force Magnitudes 26
5.2 Maximum Force Locations 27
5.3 Limitations 28
5.4 Future Work 29

CHAPTER 6 CONCLUSION 30

REFERENCES 31

APPENDIX A SUPPLEMENTAL DATA 41

APPENDIX B LOAD CELL COORDINATE TRANSFORMATIONS 42

APPENDIX C MISSING MARKER INTERPOLATION 45

CHAPTER 1

INTRODUCTION

1.1 Clinical Motivation

There are approximately 300,000 people living with spinal cord injuries (SCIs) in the United states, with 18,000 new cases of SCI each year [1]. People with spinal cord injuries (PwSCI) face many secondary complications, including an increased risk of CVD and chronic pain. As a result, about 30% of PwSCI are re-hospitalized at least once post-injury [1]. These hospitalizations and treatment plans have a huge financial impact on PwSCI and society in general: lifetime costs of care can range anywhere from $1.2 million to $5.1 million [2, 1]. A more comprehensive understanding of the causes of and ways to prevent these secondary issues is imperative to reducing the economic cost of SCIs and increasing quality of life for PwSCI.

One of the main secondary complications for PwSCI is cardiovascular disease (CVD). PwSCI represent one of the highest risk populations for developing CVD [3, 4, 5, 6, 7], which is the number one cause of premature deaths in PwSCI [8]. CVDs also occur at an earlier age in PwSCI compared to those without disabilities [9, 10].

CVD can be prevented or reduced through regular exercise [11, 12, 13], and exercise has been recommended to prevent CVD in both able-bodied and SCI populations [14]. However, SCIs affect not only mobility and function but also energy expenditure and metabolism, especially during exercise[15]. As a result, PwSCI face unique challenges with respect to heart rate and body temperature regulation during exercise. PwSCI often have to exercise at higher intensity or for a longer time to reach the same energy expenditure as able-bodied people [5]. Body temperature is also difficult to regulate during exercise for PwSCI due to reduced nervous system function[16]. This risk of overheating combined with early onset muscle fatigue makes prolonged exercise difficult for PwSCI [14]. PwSCI are also less likely to engage in physical activity compared to their able-bodied counterparts [3, 17, 4]. In

one study surveying 72 PwSCI, health conditions prevented 25% of participants from regularly exercising [18]. This is evidence of a cyclic problem in SCI populations: lack of exercise often leads to secondary health conditions, which further prevent exercise. Thus, prevention of these secondary problems is crucial for the physical and psychological health of this population. A greater understanding of how different exercise regimens affect the health of PwSCI is vital to improve the cardiovascular health and quality of life in PwSCI.

Another secondary complication for PwSCI is musculoskeletal overuse injuries. Wheelchair users (WCUs) in general are subject to higher rates of shoulder pain and injury [19, 20, 21, 22], with up to 72% reporting upper extremity pain [23]. This pain is often attributed to overuse, as the muscles and tendons in the shoulder, elbow, and wrist are subjected to new and more frequent loading as a result of wheelchair propulsion and transfers [24]. The increased loading of the upper arm during propulsion and transfers often results in degenerative morphological changes in the shoulder soft tissue [25], including rotator cuff impingement [20] and rotator cuff tendinopathy [26, 27, 28], which can be observed using magnetic resonance imaging (MRI) or clinical topography (CT) scans. Similar injury patterns are also found in wheelchair athletes, with a majority reporting upper extremity (UE) pain [29]. The high rate of soft tissue injuries in pushing sports (i.e. track and field, racing, basketball) and the direct correlation of injury rate to training time points to overuse as being one of the main causes of injury [30, 31]. Ferrara et al. found that repetitive stress/overuse injuries accounted for 35% of all injuries to elite wheelchair athletes [32]. Thus, any exercise interventions considered for preventing CVD in PwSCI must be evaluated not only for their effectiveness in improving CV health but also for their musculoskeletal safety, with an emphasis on preventing overuse injuries.

1.2 Handcycling

Handcycling, a method of propulsion that uses hand cranks attached to a chain-driven wheel, may offer a safer alternative to exercise for PwSCI compared to normal wheelchair propulsion. The gears on a handcycle offer

a greater mechanical advantage than handrim propulsion and make handcycling a more efficient alternative mode of transportation[33]. Handcycling minimizes shoulder contact forces and, by extension, upper limb soft tissue injury risk[34], without compromising energy expenditure [35]. These findings indicate that, when shoulder soft tissue injuries are a concern, handcycling may be a helpful alternative to everyday wheelchair propulsion, especially during exercise when WCUs are moving at increased speeds and power outputs.

Many handcycling biomechanics studies have examined attach-unit handcycles, with recent studies evaluating recumbent handcycles and other sport-specific variations. Attach-unit handcycles are attached to a traditional wheelchair, and the user sits in the wheelchair normally (Fig 1A). Recumbent handcycles are typically used in sport applications and feature a reclined backrest that places the body closer to the ground in a more optimal aerodynamic position (Fig. 1B). In handcycling mechanics, there are two main propulsion phases: the push phase, where the user is pushing the crank away from their body, and the pull phase, where the user is pulling the crank toward themselves (Fig. 1C). The transition from push to pull and from pull to push is characterized by a local minimum in applied tangential forces.

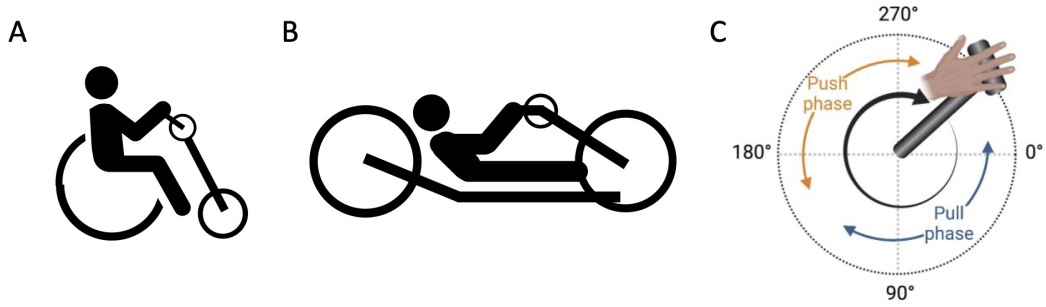

Figure 1: Handcycling configurations, including A) an attach-unit handcycle, B) a recumbent handcycle, and C) a description of the push and pull phase of handcycling.

Handcycling shows promise in reducing risk of shoulder overuse injuries in PwSCI. Thus, we chose to examine handcycling biomechanics as a potential alternative exercise mode to everyday wheelchair propulsion. While handcycling appears to be overall less physically straining on the shoulder, it's also important to consider the mode, intensity, and type of exercise that will be the most efficient in reducing CV risk in PwSCI while also not increasing

shoulder injury risk.

1.3 High Intensity Interval Training

Despite the recognized benefit of exercise for improving CV health, exercise guidelines for PwSCI still fall short in reducing CVD risk[36, 37, 5]. For example, the Canadian Physical Activity Guidelines for PwSCI [38] were found to be ineffective in reducing CVD risk factors after a 16-week exercise intervention [36]. Thus, there is a need for more well-defined exercise programs geared specifically towards improving CV health in PwSCI.

High Intensity Interval Training (HIIT), which consists of short bouts of high intensity exercise followed by periods of rest, has been identified as an exercise regimen that could effectively improve cardiovascular health in PwSCI. Typically, the high intensity intervals of HIIT fall around 80-85% VO_{2peak} and the low intensity intervals fall around 10-15% VO_{2peak}. HIIT usually requires less of an overall time commitment and is as effective as moderate intensity continuous exercise (MICT) in improving cardiovascular fitness, and therefore reducing risk of CVD, in able-bodied populations [39]. The frequent rest periods and short exercise duration in HIIT may help overcome early onset muscle fatigue prevalent in PwSCI [37, 14] making it more optimal for CV adaptations than traditional modes of continuous exercise [40]. Preliminary HIIT interventions in the SCI population have shown improved cardiovascular health [41, 42, 43]. Additionally, in a study by Astorino et. al, all SCI participants preferred higher intensity training over moderate continuous training [44]. Thus, because of the relatively low time commitment and high enjoyment rates, HIIT is a potential solution to increase exercise rates and decrease CVD in PwSCI.

Before recommending HIIT as a solution to reduce CVD risk in PwSCI, more research is needed to establish the safety of HIIT. The prevalence of UE pain and overuse injuries within wheelchair users in general [19, 20, 21, 22] raises concerns about the long-term efficacy of HIIT as an exercise intervention due to its increased intensity. Vigorous exercise, similar to the kind found during HIIT, has been associated with compromised UE health in

PwSCI [40]. Compared to the more traditional moderate intensity continuous training (MICT), HIIT has been associated with more upper body discomfort and shoulder pain [45, 46]. In a 6-week manual wheelchair exercise program, Gauthier et al. found that two out of six participants in the HIIT group experienced significantly increased shoulder pain during HIIT, and two participants were afraid of HIIT causing or increasing shoulder pain. Additionally, one participant dropped out of the HIIT group because of increased shoulder pain. This could indicate potential problems with HIIT safety and highlights the need to more closely evaluate musculoskeletal safety during HIIT for WCUs. If cardiovascular health is improved at the expense of musculoskeletal health and the comfort of wheelchair users, we may need to begin looking for another alternative or more carefully quantify the recommended duration and intensity of HIIT for SCI individuals.

1.4 Handcycling Kinetics and Reaction Forces

While handcycling is a promising exercise mode for HIIT in PwSCI, it is still important to evaluate its potential to result in soft tissue injuries, especially considering the elevated risk for WCUs. Even with the lower shoulder forces in handcycling compared to wheelchair propulsion, there is still some soft tissue injury risk associated with handcycling HIIT. Schoenmakers et al., in a 7 week able-bodied handcycling intervention study, reported significantly more upper body discomfort in those who had completed the HIIT intervention compared to MICT [45].

Our understanding of shoulder function and soft tissue injury risk can be informed by computational methods that combine in vivo biomechanical data (kinematics, kinetics) with musculoskeletal models of the body. One modeling technique involves the use of rigid-body systems based on subject-specific anthropometrics to simulate different tasks using collected kinematic and kinetic data. The outputs of rigid-body dynamics models include joint accelerations, joint torques, muscle forces, and joint contact forces[47, 48, 49, 50]. When combined with computational models at the tissue level, it is possible to obtain estimates of strains. Such models have been used to evaluate rotator cuff tears [51, 52], and have the potential to determine

whether a given exercise type may or may not place the shoulder at risk of injury.

Critical to computational analyses of shoulder biomechanics during wheelchair usage is the underlying kinetic data. Shoulder loads are largely a function of muscle and joint contact forces – which are dependent, in part, on the applied forces at the handle in the case of handcycling. In the case of handcycling, this applied force at the handcycle is the main reaction force experienced by the shoulder, and can be compared to a ground reaction force measured in legged locomotion. This ground reaction force is important in determining muscle function and joint forces and moments in walking and running[53, 54]. Therefore, the ground reaction force—or in the case of handcycling, the handle reaction force—can provide helpful insight into shoulder kinetics during handcycling and give a preliminary indication of injury risk during exercise.

Understanding how the handle reaction forces change during exercise and across various exercises can give an indication of shoulder kinetics during handcycling. Arnet et al. reported that lower hand reaction forces in attach-unit handcycling compared to wheelchair propulsion resulted in lower shoulder joint moments in attach-unit handcycling compared to wheelchair propulsion [34]. Thus, measuring applied forces at the handcycle handle can give a preliminary indication of loads experienced by the shoulder during exercise and therefore provide an indication of shoulder injury risk.

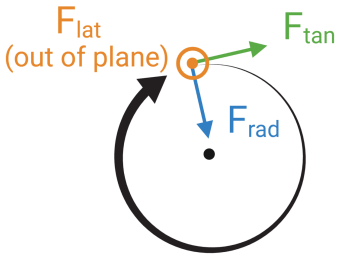

Figure 2: Force conventions used for handcycling

In this study, we report force data using polar conventions. Tangential force, the force parallel to the wheel or crank path, is positive when in the direction of rotation. Positive radial force was defined as the force pointing towards the center of the wheel or center of handcycle rotation, and lateral force, which is the force out of the sagittal plane, was defined as positive if it was pointing in the lateral direction (away from the user) (Fig. 2).

One common biomechanical measure reported during handcycling is mechanical efficiency, defined as fraction of effective force (FEF). FEF is written as

$$FEF = F_{tan}/F_{tot} \tag{1.1}$$

where F_{tot} is the total resultant applied force. Veeger et al. were the first to define FEF in the context of manual wheelchair propulsion in 1991 [55], and used it as a measure of how effective the forces applied at the wheelchair handrim were. Later, FEF was applied to handcycling[56, 57]. In handcycling, FEF can provide a similar measure of the mechanical efficiency of the applied forces at the handcycle handle. As F_{tan} is the only force component directly contributing to forward propulsion, any increase in F_{lat} or F_{rad} during exercise compared to F_{tan} would correspond to a decrease in FEF. Thus, it will be important to quantify how the forces in all three directions are changing throughout an exercise protocol to more fully understand shoulder kinetics and injury risk during recumbent handcycling exercise.

CHAPTER 2

LITERATURE REVIEW

We know that the applied torque and work distributions during handcycling change throughout a propulsion cycle[58, 59]. Therefore, continuous kinetic data is important to examine as it can give us a more complete picture of the loads experienced by the shoulder throughout an entire propulsion cycle. Understanding the location of maximum applied forces during a propulsion cycle can give an indication of propulsion positions where the loads experienced by the shoulder are the highest.

While many studies have reported discrete (e.g. minimum, maximum and average) applied forces during both attach-unit and recumbent handcycling, fewer have examined and reported continuous kinetics during handcycling, and no studies have reported three-dimensional applied forces during recumbent handcycling (Table 1). Other studies were excluded because the force data was not split into a propulsion cycle[60, 61, 62], was not reported numerically[34, 63, 64, 59] or was not in the tangential, radial, and lateral coordinate system[65].

Table 1: Studies reporting continuous kinetic data during handcycling. Abbreviations: N-D (Non-disabled participants), SCI (spinal cord injury), AMP (amputee), CP (cerebral palsy), AUHC (attach-unit handcycling), RHC (recumbent handcycling)

Paper	Participants	N	Mean Age (years)	Exercise	Measurements	Summary
Kraaijenbrink et al., 2017[66]	N-D	12	23.9	AUHC	F_{tan}	1.94 m/s
Kraaijenbrink et al., 2020[67]	N-D	12	23.9	AUHC	F_{tan}, F_{rad}, F_{lat}	1.94 m/s
van Drongelen et al., 2011[68]	SCI	1	Not reported	AUHC	F_{tan}, F_{rad}, F_{lat}	25, 35, 45, 55, and 65 W at 1.67 m/s
Jakobsen and Ahlers, 2016[69]	N-D	1	26	RHC	F_{tan}	Self-selected speed
Mason et al., 2021[70]	5 SCI, 2 AMP, 2 CP	9	33.2	RHC	Torque	70% PPO at 4 crank lengths
Quittmann et al., 2018[71]	N-D	12	26	RHC	Torque	20, 40, 60, 80, 100, 120W
Quittmann et al., 2020[72]	N-D	12	26	RHC	Torque	Sprinting
Vegter et al., 2019[58]	N-D	12	25	RHC	Torque	30 and 60 W at 4 crank fore-aft positions

2.1 Attach-Unit Handcycling

Three studies have reported continuous applied forces during attach-unit handcycling[68, 66, 67], with two studies [68, 67] reporting all three force components. The tangential force profiles have similar shapes and primarily differ in the magnitude of the forces (Fig 3). The largest peak tangential force recorded was 45 Newtons and occurred between 64° and 91° of the cycle (Fig 3). The transition from push to pull phase is indicated by the local minimums of tangential forces which occurred between 276° and 310°. As rolling resistance increased, tangential forces also increased to maintain speed[66]. Able-bodied subjects cycling at 1.94 m/s had lower tangential forces[66, 67] than those reported in a subject with paraplegia cycling at 35W [68].

Multiple other studies recorded continuous applied forces but did not report them. Abassi Bafghi et al. reported average force magnitudes in the

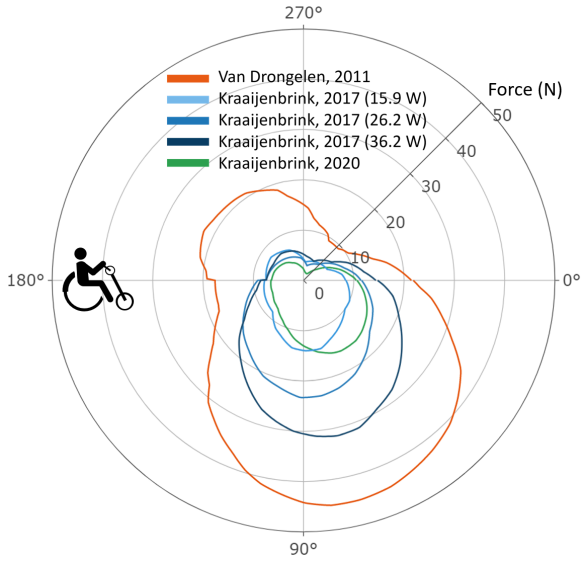

Figure 3: Tangential force (N) during attach-unit handcycling[68, 66, 67]. The three shades of blue represent crank propulsion for different rolling resistance levels within the same study, measured in Watts. As resistance increases, the shade of blue darkens.

sagittal plane and lateral direction over 30 seconds of handcycling for four different speeds[56]. Three other studies used continuous applied forces during handcycling for inverse dynamics models but did not report them[64, 34, 63].

Other studies have reported FEF during a propulsion cycle in attach unit handcycling[57, 73, 66, 74]. FEF values have ranged from around 50%[66] up to 83%[73], all at submaximal speeds.

2.2 Recumbent Handcycling

While researchers have studied the biomechanics of attach-unit handcycling, less is known about the biomechanics of recumbent handcycling. As recumbent handcycles are the main handcycling mode used in sport and exercise applications, it is important to understand the specific biomechanics of recumbent handcycling to predict and prevent soft tissue injuries during exercise in WCUs.

To my knowledge, only one study has reported direct measurements of continuous applied forces during recumbent handcycling (Fig 4A)[69]. Jakobsen and Ahlers report a maximum tangential force of 127 N at 107° in the propul-

sion cycle, with a pronounced push-pull and pull-push transition at 2° and 199°, respectively. Several studies have investigated the effect of changing either the handcycle configuration (i.e. crank length, backrest angle, crank position, etc.) or the power output during propulsion and reported continuous torque during recumbent handcycling[71, 72, 70, 58]. This torque data can be used to indirectly calculate F_{tan} using Equation 2.1:

$$F_{tan} = \tau / R \tag{2.1}$$

where τ is the torque at the crank and R is the crank length. Changes in crank

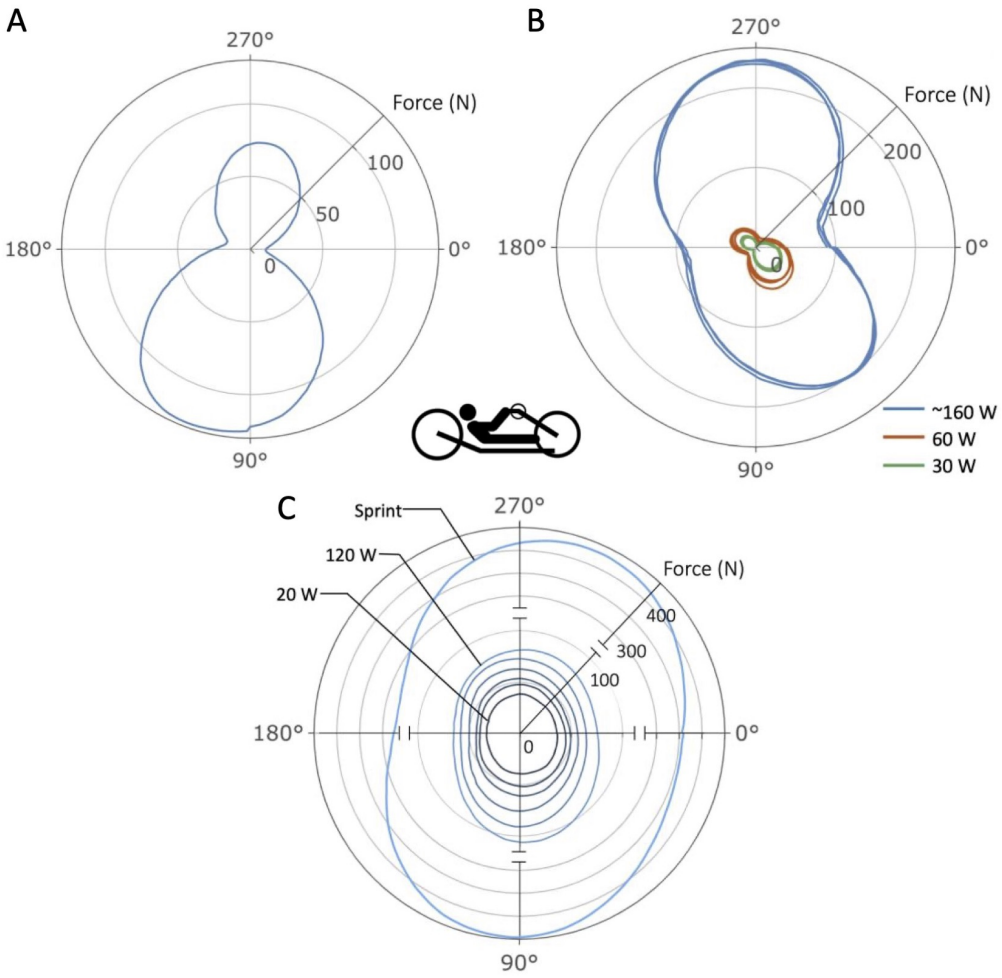

Figure 4: Tangential applied force (F_{tan}) (N) during recumbent handcycling. Studies examining A) F_{tan} measured directly using a strain gauge-instrumented handle, self-selected speed[69], B) changes in handcycle configuration (changes in crank length shown in blue[70], and changes in crank fore-aft position, as a percentage of arm length, shown in orange and green[58]) and C) changes in power (20-120W)[71] and sprinting[72].

length do not significantly change the applied torque profiles[70] (Fig 4B, blue lines). However, torques are sensitive to the crank position[58]: when the crank is moved closer to the participant, the torque in the push phase increases and torque in the pull phase decreases (Fig 4B). The tangential forces during recumbent handcycling kinetics are also sensitive to changes in power output with maximum force increasing with increasing power.

The location of maximum force across studies was variable (range = 34° - 273°), and could be a result of varying levels of handcycling experience, handcycle design, participant demographics, and different methodologies in collecting force data. The location of the push-pull transition (291°-2°) and pull-push transition (132°-199°) (Fig 1C), defined as the location of minimum applied force, were more consistent across studies though studies investigating the effect of power (Fig 4C) did not report a clear transition point. Compared to attach unit handcycling, the push-pull transition occurs later in the propulsion cycle. It is worth noting that the study directly measuring F_{tan} (Fig 4A) has a force profile similar to that recorded during attach unit handcycling, with the maximum tangential force occurring at the bottom of the propulsion cycle (Fig 3). It's possible that, with more consistent data collection methods across recumbent and attach-unit handcycling, a clearer tangential force curve would emerge.

While these changes in handcycling configuration result in slightly different torque profiles during handcycling, it appears that recumbent handcycling kinetics are most obviously affected by changes in power output. As the power output of the handcycle increases, the maximum tangential force per cycle increases linearly ($R^2 = 0.8$) (Fig 4A and B). Therefore, the most important consideration for injury potential may be exercise intensity.

To my knowledge, only one study has examined FEF in recumbent handcycling. Faupin et al. investigate the impact of changing backrest angle and handcycle configurations on FEF and reported mean FEF between 85.1% and 89.3%, with a more upright backrest position resulting in lower efficiency[75]. However, this FEF did not include lateral forces in the F_{tot} calculation, and could be overestimating the true 3-dimensional FEF. This paper also only reported discrete values. As a result, more must be done to quantify continuous 3-dimensional force application effectiveness throughout a cycle in

recumbent handcycling.

2.3 Remaining Questions

The question remains as to which power or speed levels, and for how long, are acceptable to avoid overuse injuries common in WCUs. During sprinting, the tangential applied forces reach a maximum of 447 N (Fig. 4C), which is more than ten times larger than the maximum tangential forces reported during attach-unit handcycling (Fig. 3). When PwSCI train at increased speeds and power outputs, it is reasonable to suggest that these increased external forces will result in increased loads at the shoulder. It is also unclear specifically how HIIT affects kinetics, and therefore shoulder mechanics and injury risk, of PwSCI. While HIIT is hypothesized to be less physiologically fatiguing than MICT due to the frequent rest periods[37, 14], it is unknown if HIIT is also less mechanically straining than MICT.

Table 2: Studies examining handrim or handcrank kinetics during fatigue in wheelchairs and handcycles. Abbreviations: N-D (Non-disabled participants), SCI (spinal cord injury), WP (wheelchair propulsion), RHC (recumbent handcycling)

Paper	**Exercise type**	**Partic-ipants**	**N**	**Fatigue Protocol**	**Kinetic results**
Rodgers, 1994[76]	WP	SCI	20	Graded exercise test (increasing resistance) to exhaustion	Increased peak total handrim force
Rice, 2009[77]	WP	SCI	21	10-min propulsion trial at 1.4 m/s	Decreased max F_{lat}, no change in other forces
Qi, 2012[78]	WP	N-D	14	Continuous tests to fatigue at 0.9 and 1.6 m/s	No significant change in forces
Quittmann, 2018[71]	RHC	N-D	12	Incremental step test (increasing power output) to exhaustion	Increased max and min crank torque, Work shifted from push to pull phase, No change in location of max torque
Quittmann, 2020[79]	RHC	N-D	12	30-min continuous test at lactate threshold	Decreased max and min crank torque, Work shifted from push to pull phase

The effects of fatigue in general on applied forces during handcycling are unclear, as kinetic fatigue studies in handcycling—and wheelchair propulsion in general—are limited (Table 2). To my knowledge, only 3 studies have examined change in applied forces during fatigue protocols in wheelchair propulsion, and the results vary depending on the fatigue protocols. Results vary from decreased F_{lat}[77] to increased total handrim force[76] to no change in kinetics at all[78]. Only 2 studies have examined the kinetics of fatigue during handcycling, and found that the percentage of work completed during the push phase decreased while the percentage of work during the pull phase increased[71, 79]. Depending on the fatigue protocol, crank torque increased or decreased, while the crank angle of the maximum torque during propulsion remained the same. However neither of these studies reported 3-D crank kinetics, so it is still unclear how the force components change as a result of fatigue.

Only continuous F_{tan} data was available in the literature for recumbent handcycling, despite the importance of 3-dimensional force information in predicting shoulder musculoskeletal loads[80, 81]. It's still unclear how the other components (radial and lateral) are impacted by changes in recumbent handcycle configurations and power. Two studies examined 3-dimensional applied forces in attach-unit handcycling[67, 68]. Van Drongelen et al. reported that the tangential force was the largest (over 40 N magnitude), followed by the radial applied force (around 20 N). They also found that the applied force in the lateral direction was the smallest, staying under 20 N during a single propulsion cycle[68]. Similarly, Kraaijenbrink et al. reported F_{lat} values between -10 and 10 N and larger F_{tan} and F_{rad} values between -10 and 20 N[67]. We would expect similar force patterns in recumbent handcycling, but more research is needed to confirm these trends as recumbent handcycling involves altered body positioning and kinematics compared to attach-unit handcycling[82].

It is also unclear how the FEF, which is an indication of propulsion effectiveness, changes throughout a HIIT exercise protocol. In low intensity attach-unit handcycling, the FEF decreases as speed increases[73], but no studies have reported FEF during high intensity handcycling. Fatigue studies in handcycling (Table 2 only examined torque at the crank, so fatigued FEF handcycling measurements are not available. Changes in FEF during

legged-biking due to fatigue are inconclusive [83], but it is unclear how well legged-cycling translates to arm-powered handcycling. Decreases in FEF due to increased F_{rad} or F_{lat} applied forces could be participants compensating to reduce shoulder strain, as 100% F_{tan} during normal wheelchair propulsion (FEF = 1) actually increases physiological cost[80]. Understanding how FEF changes during HIIT and MICT can give a preliminary indication of how shoulder loading, and therefore shoulder soft tissue injury risk, is changing throughout an exercise protocol.

Force changes for all three directions are important for modeling the upper extremities and understanding musculoskeletal loads during any activity, including recumbent handcycling. Thus, the purpose of this study was to characterize kinetic profile differences in recumbent handcycling during HIIT and MICT. We measured three-dimensional applied forces at the crank handle during recumbent handcycling in both HIIT and MICT exercise regimens in WCUs. Using this data, we analyzed the location of maximum total applied forces and maximum tangential, radial, and lateral forces to determine locations of interest for preventing shoulder soft tissue injuries.

CHAPTER 3

METHODS

This study was approved by the Institutional Review Board at the University of Illinois and all testing was performed at the Wheelchair Biomechanics Lab.

3.1 Participants

Twenty-one participants were recruited from the University of Illinois adapted sports teams. Inclusion criteria were 1) age 18-45, 2) at least 12 months post onset of neurologically stable spinal cord injury or spinal cord dysfunction, 3) participated in vigorous intensity exercise in the last 30 days, and 4) met the American College of Sports Medicine (ASCM) minimum physical activity recommendations[84]. If individuals exhibited signs or symptoms of CVD, regular upper extremity pain, or other conditions or injuries preventing them from safely participating in sports activities, they were excluded from the study. Participants completed a demographic survey where sex, age, height, weight, and years with disability data was recorded.

3.2 Exercise Protocols

Prior to each session, participants were asked to refrain from strenuous exercise, caffeine, and alcohol for 24 hours[84]. All exercises were completed on a recumbent handcycle (Top End, Invacare, USA). The handcycle was adjusted to each participant such that at the maximal reach phase the elbows were flexed between 15 and 20°, which has been shown to maximize power production[85].

Participants completed three exercise sessions (Table 3) beginning with an incremental test to exhaustion[45] wherein participants began cycling at

Table 3: Exercise Protocols completed by participants. Abbreviations: HIIT (High intensity interval training), MICT (Moderate intensity continuous training), PO (power output), PPO (peak power output)

Session	Protocol	PO
1	Incremental test to exhaustion	30 W, increase by 10 W every minute
2	High intensity interval training	1 min at 90% PPO 1 min at 10% PPO 10 total intervals
3	Moderate intensity interval training	45% PPO

30 W after which power was increased by 10 W every minute until they voluntarily stopped cycling or were no longer able to maintain the selected power output. Power output was collected at 2Hz using a powermeter (SRM, Julich, Germany) attached to the handcycle hub. Each participant's peak power output (PPO) was calculated as:

$$PPO = P_{max} + (t * 10W) \tag{3.1}$$

where P_{max} was the final PO the participant was able to complete for 60 seconds and t was the time (in minutes) that participants cycled into the next interval before stopping. After the incremental test, participants remained on the handcycle for 8-10 minutes to recover, either by handcycling slowly or resting. Once participants were recovered, they completed a HIIT familiarization routine, which involved one interval of the HIIT protocol (Table 3)[44, 86].

The second exercise session was a HIIT session which consisted of 10 intervals of high and low-intensity exercise. For each interval, participants cycled for one minute at 90% PPO, followed by one minute at 10% PPO[86, 87].

The third session, MICT, involved participants cycling at 45% PPO[88] until the work done during MICT matched the work completed during HIIT. Total work, W_{total}, was calculated by integrating the power-time curve using a trapezoidal sum in MATLAB (Mathworks, Natick, USA) from which the time for the MICT session (t_{MICT}) was calculated as:

$$t_{MICT} = W_{total}/(0.45 * PPO) \tag{3.2}$$

where PPO was the participant's peak power output, calculated in Eq. 3.1.

After both the HIIT and MICT sessions, participants were given 5-10 minutes in the handcycle to rest and recover before leaving the testing site. Each session was completed within 2-7 days of the previous session.

3.3 Handcrank Kinetics

Applied forces at the right hand crank were collected during both the HIIT and MICT sessions at 2000 Hz using a custom handle instrumented with a six-axis load cell (ATI, Apex, USA). The angle of the crank and handle were measured using five reflective markers placed on the handle and crank (Fig. 5A). Marker motion was recorded at 100 Hz using a 10-camera Vicon Nexus motion capture system (Vicon Motion Systems, Yarnton, UK).

Synchronous force and crank/handle motion data were collected during the 1^{st}, 3^{rd}, 5^{th}, 7^{th}, 9^{th}, and 10^{th} HIIT high intensity (90% PPO) intervals. Similarly, data was collected at 6 timepoints during the MICT session that matched the workloads at the 6 HIIT collection timepoints.

3.4 Data Analysis

Data processing was completed in MATLAB. Kinetic data was filtered using a 2^{nd} order low-pass Butterworth filter with a cutoff frequency of 10 Hz. We identified the first ten propulsion cycles at each time point using the recorded motion data, denoting 0° as the most distal (furthest away from the user) crank position. The local load cell x, y, and z-coordinate system was converted to the tangential (F_{tan}), radial (F_{rad}), and lateral (F_{lat}) handcycle coordinate system using the marker positional data (Fig. 5B). We extracted the maximum forces in the tangential, radial, and lateral directions and the

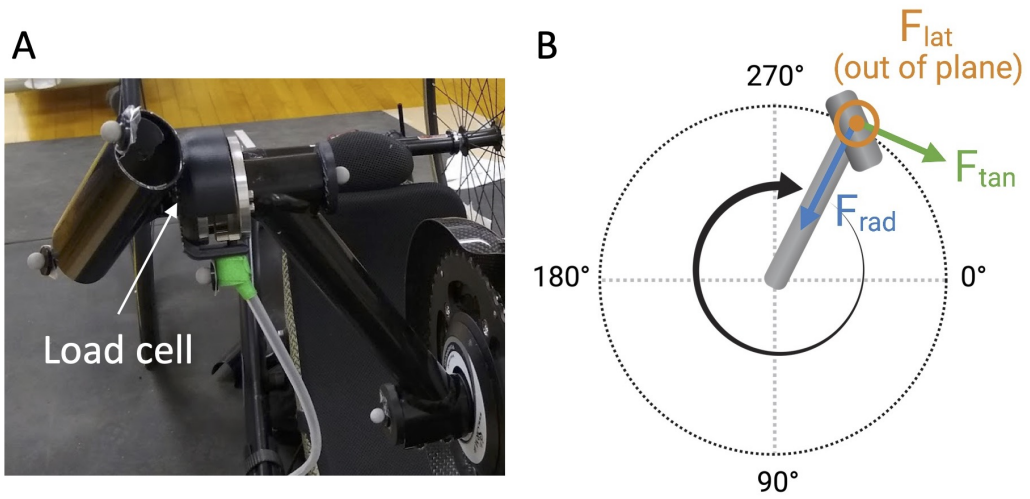

Figure 5: A) Handcycle handle instrumented with the six-axis load cell and with 5 markers attached to track crank angle and handle movement. B) Handcycle angle and force conventions used in this paper, with the 0° position being the furthest away from the body. F_{tan} is positive when pointing in the direction of rotation, positive F_{rad} is radially inward, and positive F_{lat} is pointing in the lateral direction (away from the participant).

corresponding location of maximum force during the rotational cycle for each participant at each timepoint was analyzed.

3.5 Statistical Analysis

Statistical analysis was completed in RStudio (Boston, USA). Variables were tested for normality using a Shapiro-Wilk test. Since some variables were not normally distributed, a Wilcoxon signed-ranks test was used to compare the maximum forces and maximum force locations between HIIT and MICT at the same timepoint and between timepoint 1 and timepoints 2-6 within the same exercise test.

CHAPTER 4

RESULTS

Due to a malfunction with the load cell during testing, force data from timepoint 3 of participant 18's MICT protocol was excluded as well as the corresponding HIIT data.

4.1 Participants

Twenty-one participants were recruited (Table 4). One person dropped out after Session 1 (incremental test) due to health reasons unrelated to the study and their data was excluded. Twenty participants completed all 3 exercise tests. No adverse events or injuries were recorded during or after exercise testing.

Table 4: Participant Demographics. Data are mean± SD.

n	**Sex**	**Age (years)**	**BMI**	**Years with disability**	**PPO (W)**
20	9 f 11 m	25.50 ±6.83	22.66 ±4.47	20.42 ±6.20	136.33 ±36.67

Participants all had either a spinal cord injury (n=8), or spinal cord dysfunction (spina bifida n=8, transverse myelitis n=3, and cauda equina syndrome n=1). All participants used wheelchairs as their main mode of transportation.

4.2 Maximum Force Magnitudes

The maximum tangential, radial, and lateral forces for each participant at each timepoint were calculated during both HIIT vs. MICT and used to analyze the differences in the distribution of force magnitudes. During

both exercise protocols, tangential forces were the largest followed by radial and then lateral (Fig 6 A-C). For all three force components, HIIT forces were significantly different than those of maximum MICT forces at every timepoint. The maximum tangential forces during HIIT were 54.2% higher than MICT forces ($p<0.001$, Table 5). Similarly, the maximum radial forces were 38.0% higher in HIIT than MICT (p-range = 0.001-0.05). While lower in magnitude, the maximum lateral forces were 63.9% higher in HIIT compared to MICT ($p<0.001$).

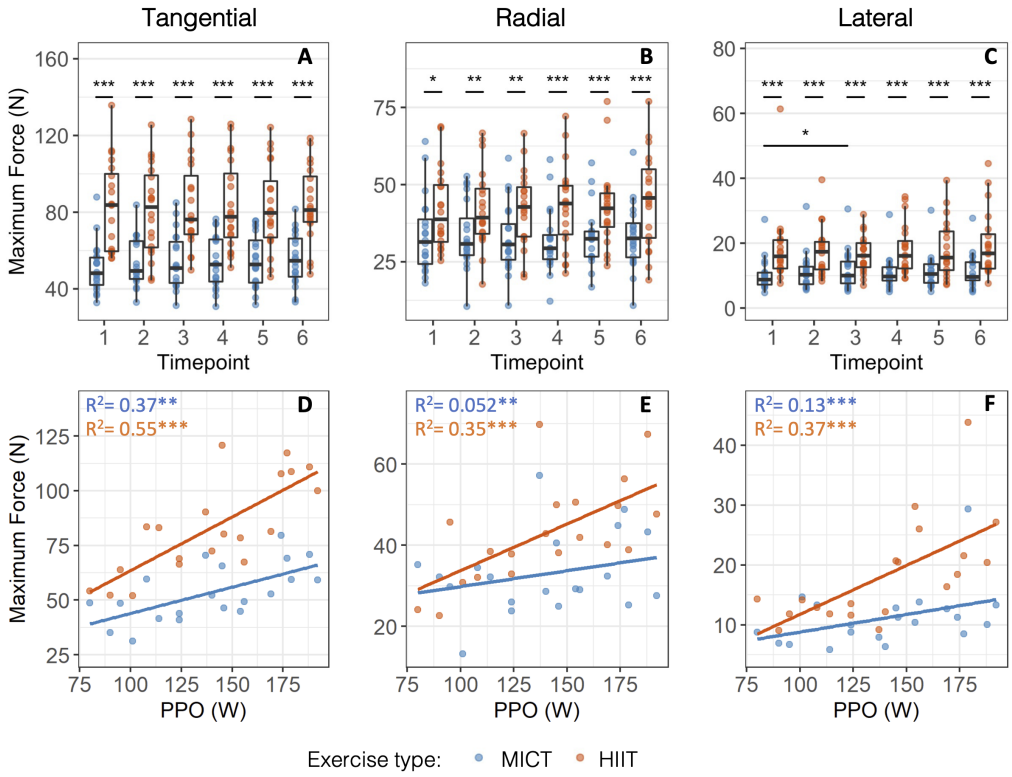

Figure 6: Maximum forces in a propulsion cycle. Values of maximum tangential forces (left column), radial forces (center column) and lateral forces (right column) are plotted on the top row (graphs A, B, and C). The relationship between the average maximum forces for each participant compared to their peak power output (PPO) are plotted on the bottom row. *p<0.05, **p<0.01, ***p<0.001

Table 5: Maximum force component magnitudes at each timepoint for each exercise protocol. Data are median (median absolute deviation). * denotes significantly different distributions from MICT timepoint, where *p<0.05, **p<0.01, ***p<0.001. ^{a} indicates significantly different distributions from timepoint 1 of the same exercise protocol, where ^{a} is p<0.05.

	Timepoint					
	1	**2**	**3**	**4**	**5**	**6**
F_{tan} (N)						
MICT	48.2 (11.3)	49.0 (12.9)	50.8 (14.8)	52.7 (18.2)	52.8 (16.1)	54.7 (15.6)
HIIT	83.7 (34.5)***	82.7 (29.5)***	76.2 (23.7)***	77.6 (25.5)***	79.7 (19.8)***	81.1 (17.1)***
F_{rad} (N)						
MICT	31.4 (10.8)	30.8 (6.8)	30.6 (8.2)	29.4 (5.9)	32.4 (8.2)	32.6 (9.5)
HIIT	38.8 (14.3)*	39.3 (10.2)**	42.8 (14.2)**	43.9 (10.3)***	42.3 (8.2)***	45.7 (17.7)***
F_{lat} (N)						
MICT	8.8 (2.7)	10.3 (4.5)	10.0 (5.4)^{a}	9.7 (3.8)	10.5 (4.5)	9.6 (5.2)
HIIT	15.9 (6.5)***	17.4 (7.0)***	16.1 (5.9)***	16.1 (6.0)***	15.6 (8.8)***	16.9 (7.5)***

There were no significant differences in maximum forces from timepoint 1 through the rest of the protocol. The sole exception occurred in the maximum lateral forces during MICT which differed between timepoint 1 and timepoint 3 (p=0.014) by 1.2 N. The amount of maximum force generated during handcycling was correlated to the peak power output based on the prescribed power levels for both HIIT and MICT (Fig 6 D, E, and F). The amount of variation in maximum force that could be explained by peak power output was higher in HIIT (R^2 range = 0.35-0.55, p<0.001)) compared to MICT (R^2 range = 0.052 to 0.37, p<0.01).

4.3 Maximum Force Locations

There were two peaks in tangential force profiles during handcycling reflective of the pull phase (first peak) and push phase (second peak) during the propulsion cycle (Fig 7A). The tangential forces were positive during the propulsion cycle. There was no difference in the location of the first peak of the tangential forces during HIIT (average = 57.0°) compared to MICT (average = 53.5°) and peak location did not change during the course of exercise (Fig 7D), p-range = 0.07-0.96). Similarly, the location of the second tangential peak force was not significantly different between HIIT and MICT with the exception of timepoint six with a shift of 6° in HIIT (p = 0.029, Table 6). Overall, there were no significant differences during the course of exercise for either peak except for a 1° shift in MICT peak 2 between timepoints 1 and 2.

The radial forces were both positive and negative during a single propulsion cycle and were described by multiple peaks with a maximum radial force at 337.5-360.0° and a minimum radial force at 103.5-112.0° (Fig 7B) during both HIIT and MICT, which correspond to push towards the crank axis and away from the crank axis, respectively. The maximum radial force (noted as Peak 1) occurred at 340° in MICT and 349.0° in HIIT (Fig 7E). The maximum radial force during timepoint six occurred 16° later in HIIT compared to MICT (p = 0.04, Table 6). The minimum radial force (Peak 2) occurred on average at 106.0° in MICT and 108.0° in HIIT with a 4.5° shift in HIIT compared to MICT at timepoint 4 (p = 0.02). There was no difference in radial force locations during the course of exercise for either MICT or HIIT.

Table 6: Peak force locations at each timepoint for each exercise protocol. Data are median (median absolute deviation). * denotes significantly different distributions from MICT timepoint, where *p<0.05, **p<0.01, ***p<0.001. [a] indicates significantly different distributions from timepoint 1 of the same exercise protocol, where [a] is p<0.05.

		Timepoint					
		1	**2**	**3**	**4**	**5**	**6**
F_{tan} (°)							
Peak 1	MICT	53.5 (11.9)	54.5 (19.3)	52.5 (14.8)	55.0 (16.3)	51.5 (17.8)	51.5 (16.3)
	HIIT	58.5 (19.3)	56.5 (14.8)	54.0 (13.3)	57.5 (14.1)	59.0 (13.3)	56.5 (20.0)
Peak 2	MICT	220.0 (17.8)	**219.0 (20.8)**[a]	219.5 (16.3)	219.0 (14.1)	219.5 (16.3)	217.0 (14.8)
	HIIT	220.0 (8.9)	224.5 (8.2)	224.0 (10.4)	225.0 (12.6)	222.5 (11.9)	**223.0 (13.3)***
F_{rad} (°)							
Peak 1	MICT	337.5 (17.8)	340.0 (16.3)	339.5 (11.9)	340.5 (13.3)	337.5 (17.0)	344.0 (22.2)
	HIIT	353.0 (44.5)	341.0 (28.9)	351.0 (43.0)	343.5 (24.5)	350.0 (36.3)	**360.0 (32.6)***
Peak 2	MICT	108.0 (20.0)	107.0 (19.3)	106.5 (16.3)	105.0 (13.3)	104.5 (16.3)	103.5 (14.1)
	HIIT	111.5 (34.1)	108.5 (21.5)	108.0 (17.8)	**109.5 (14.1)***	107.0 (17.0)	112.0 (22.2)
F_{lat} (°)							
Peak 1	MICT	165.0 (91.2)	149.5 (97.1)	167.0 (112.7)	141.0 (57.8)	142.5 (61.5)	152.0 (74.1)
	HIIT	145.5 (99.3)	141.0 (57.8)	139.0 (84.5)	146.0 (68.2)	148.0 (78.6)	128.5 (32.6)

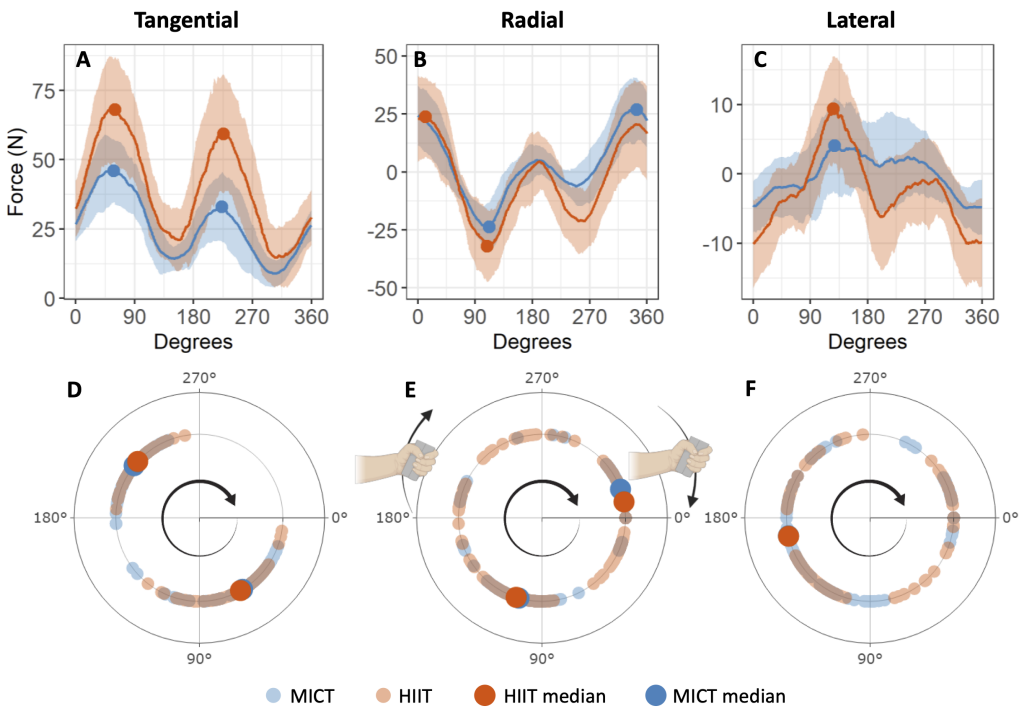

Figure 7: Median profiles for A) tangential force, B) radial force, and C) lateral force for HIIT and MICT. Points of interest (maximum and minimum peaks) are indicated with a dot, and the median absolute deviation at each timepoint is shaded. Median location of points of interest for D) tangential, E) radial, and F) lateral forces for all timepoints during both HIIT and MICT protocols. The median location is indicated with a larger dot.

The lateral force magnitude tended to have one peak (Fig 7C). While not significantly different, HIIT lateral forces peaked 8.3% earlier in the propulsion cycle than MICT lateral forces (Table 6). Similarly, there were no differences between HIIT and MICT lateral forces within timepoints or between timepoint 1 and future timepoints (Fig 7F).

CHAPTER 5

DISCUSSION

Overall, the maximum applied forces were larger in HIIT compared to MICT, and there were some changes in the location of these maximum forces in HIIT compared to MICT towards the end of the protocols. There was very little change in the value and location of the maximum forces in timepoint 1 compared to subsequent timepoints within HIIT or MICT.

5.1 Maximum Force Magnitudes

We observed a large amount of inter-participant variation in the maximum forces at each timepoint, which is likely due to the design of our exercise protocol which used a participant-specific intensity level for peak power output (PPO). The target power output during HIIT and MICT was a significant correlate of the maximum forces reached during a propulsion cycle and more so during HIIT compared to MICT for all force components (Fig 6 D-F).

Despite this variation, the tangential component was consistently the largest of the three components in agreement with data from others [68]. Importantly, all participants were able to complete the exercise protocol. There was no change in the maximum forces between timepoint 1 and timepoints 2-6 during a protocol, except for the lateral forces in MICT timepoint 3. Participants were able to maintain the same force output during both the HIIT and MICT protocol suggesting that neither protocol results in musculoskeletal fatigue to the point where participants could no longer maintain their intended power output. These results are promising for HIIT to serve as a potential exercise for challenging the cardiovascular system in a sustainable manner.

While the radial and lateral force components during handcycling do not contribute to forward motion, they are unavoidable forces during handcyling. We found that the radial forces were nearly half as large as the tangential

forces. From a training perspective and mechanical efficiency of handcycling, it would be desirable to eliminate or minimize this radial force since it does not contribute to forward propulsion. However, it is unclear how this applied force at the handle translates to and affects shoulder contact forces and joint moments. Bregman and colleagues suggested that the non-tangential forces are important in reducing the glenohumeral contact forces in everyday wheelchair propulsion[80] based on their finding that applying 100% tangential forces increases shoulder moments[80]. It is still unknown whether the non-tangential forces should be minimized to increase propulsion efficiency, or if they should be encouraged to lower joint moments and therefore shoulder injury risk.

In comparing HIIT to MICT, it was clear that HIIT required larger forces. The tangential forces were almost double in HIIT versus MICT and it is therefore likely that handcycling during HIIT results in larger forces within the shoulder compared to MICT. Importantly, no subjects reported pain and all were able to complete both the HIIT and MICT protocols. Whether or not a longitudinal exercise protocol involving HIIT would result in musculoskeletal injury is unknown. However, we believe the use of a participant-specific targeted power output level is one mechanism for mitigating the potential for overuse injuries during exercise.

5.2 Maximum Force Locations

The location of maximum tangential and radial forces during handcyling was different at the end of exercise when comparing HIIT to MICT, which suggests that the kinematics of handcycling changed at the end of the exercise protocols. It's possible that participants were experiencing some fatigue during the protocols but this remains to be confirmed. The maximum positive radial force, which corresponds to the participant pulling the most towards the center of the crank, occurred between 340-349° for both HIIT and MICT. At this location the arm is almost fully extended in the handcycle and could be a potential point for investigation, as other sports where the arm is in an overhead position are known to put the shoulder at increased risk for injury[89]. In the case of handcycling, this location will result in a

maximum moment arm of the applied forces exerted on the handle about the shoulder. The potential differences in kinematics should be investigated further using motion capture or inverse dynamics techniques. Understanding how propulsion style changes throughout the exercise protocol can give a better understanding into ways to improve propulsion, reduce injury risk, or recommend other exercise techniques to PwSCI.

There were several outliers in radial force patterns that resulted in two groups of peak radial forces: one at 200° and another at 250° (Fig 8). When these 60 data points were removed, there was a significant ($p<0.05$) difference in the first peak radial force location from MICT to HIIT in timepoint 1, 5, and 6 ($p = 0.03$, 0.008, and 0.01, respectively). There was no significant difference in the distribution of the location of radial peak 2 in HIIT compared to MICT with the extraneous points removed. Interestingly, peak 1 of the radial forces is also the peak that occured when the arm was fully extended (around 360° in the propulsion cycle). With a larger sample size or training to more uniformly correct propulsion technique, these inter-participant variations in radial force profiles could be minimized to more accurately characterize changes in force profiles during exercise.

5.3 Limitations

While examining the kinetics of handcycling during HIIT and MICT can give a preliminary idea of the loads experienced by the shoulder during exercise, they are not a direct measurement of shoulder contact forces or joint moments. Thus, it is difficult to know the degree to which hand forces contribute to shoulder loading and therefore injury risk. However, Arnet reported that lower hand reaction forces in attach-unit handcycling compared to wheelchair propulsion resulted in lower shoulder joint moments[34]. Measuring applied forces at the handcycle handle can therefore give a preliminary indication of loads experienced by the shoulder during exercise and provide an early indication of shoulder injury risk.

The power-based design of the exercise protocol inherently introduces inter-participant variability. Rather than having all participants handcy-

cle at the same power output, the exercise protocols were catered to each individual and their fitness level. This was to ensure that the effort levels were similar across participants for each protocol, but did introduce variability in the target PO levels for each exercise. Thus, our analysis of the hand kinetics during handcycling should be interpreted carefully - and that the variation we report is an artifact of the design and not necessarily the degree of variability in forces during handcycling in general.

Finally, the participants recruited for this study were all members of the University of Illinois adapted sports teams. Because of this, their exercise rates and fitness levels are likely higher than the average SCI population. We would expect any differences in propulsion style and fatigue observed in these highly trained individuals would be heightened in untrained populations, and thus the differences in propulsion kinetics found in this study would still apply.

5.4 Future Work

We have observed some changes in the location of maximum forces between HIIT and MICT towards the ends of the exercise protocols. While this could be indicating altered kinematics that result in different force application patterns, it's difficult to pinpoint exactly where this difference in force profiles is originating from. Quantifying changes in kinetics of handcycling during exercise is a necessary start, but to understand how these forces translate to joint contact forces, joint moments, and muscle forces, musculoskeletal models should be used. Combining these continuous force measurements with kinematic (motion) data will allow for the creation of inverse dynamics models that can directly compute joint angles, joint contact forces, and joint moments. These models would allow for a more specific determination of the propulsion locations and techniques that are putting the shoulder at greatest risk for injury. With this information, we can more completely characterise the biomechanics of handcycling exercise in PwSCI and work to improve propulsion techniques and reduce injury risk.

CHAPTER 6

CONCLUSION

Handcycling HIIT is associated with higher maximum applied forces in all 3 force directions compared to MICT. These applied forces, when viewed as an early indication of shoulder joint loading, may indicate that HIIT is associated with higher shoulder contact forces than MICT. Additionally, changes in the location of peak forces (specifically, tangential peak 2 and radial peak 1) may point to altered kinematics from MICT to HIIT at the end of the protocol, potentially due to muscle fatigue. These differences should be investigated to more fully characterize changes in joint angles during propulsion. With this information, we hope to begin to evaluate injury risk during handcycling HIIT.

While exercise for PwSCI is important to reduce risk of CVD and improve quality of life, it is still unclear exactly how to balance the need for improved exercise techniques and routines while still reducing risk of injury. Any exercise regimen recommended for PwSCI must also be evaluated for musculoskeletal safety, as high shoulder soft tissue injury rates in PwSCI are a major concern. Understanding how the applied forces at the handle are changing through a propulsion cycle and throughout an exercise protocol can inform training techniques, exercise development, and safety measures. This information, combined with kinematic data and musculoskeletal modeling, can be used to directly calculate shoulder contact forces, moments, and muscle forces, and therefore predict injury risk during exercise.

REFERENCES

[1] National Spinal Cord Injury Statistical Center, "Spinal cord injury facts and figures at a glance." pp. 1–2, 2021.

[2] M. J. DeVivo, Y. Chen, S. T. Mennemeyer, and A. Deutsch, "Costs of care following spinal cord injury," *Topics in Spinal Cord Injury Rehabilitation*, vol. 16, no. 4, pp. 1–9, 2011.

[3] R. A. Washburn, W. Zhu, E. McAuley, M. Frogley, and S. F. Figoni, "The physical activity scale for individuals with physical disabilities: Development and evaluation," *Archives of Physical Medicine and Rehabilitation*, vol. 83, no. 2, pp. 193–200, 2002.

[4] K. A. Martin Ginis, K. P. Arbour-Nicitopoulos, A. E. Latimer, A. C. Buchholz, S. R. Bray, B. C. Craven, K. C. Hayes, A. L. Hicks, M. A. McColl, P. J. Potter, K. Smith, and D. L. Wolfe, "Leisure Time Physical Activity in a Population-Based Sample of People With Spinal Cord Injury Part II: Activity Types, Intensities, and Durations," *Archives of Physical Medicine and Rehabilitation*, vol. 91, no. 5, pp. 729–733, 2010.

[5] R. A. Tanhoffer, A. I. Tanhoffer, J. Raymond, A. P. Hills, and G. M. Davis, "Exercise, energy expenditure, and body composition in people with spinal cord injury," *Journal of Physical Activity and Health*, vol. 11, no. 7, pp. 1393–1400, 2014.

[6] S. N. Blair, "Physical inactivity: The biggest public health problem of the 21st century," University of Southern California, Tech. Rep. 1, 2009. [Online]. Available: http://bjsm.bmj.com/

[7] J. P. Thyfault and R. Krogh-Madsen, "Metabolic disruptions induced by reduced ambulatory activity in free-living humans," *Journal of Applied Physiology*, vol. 111, no. 4, pp. 1218–1224, 2011.

[8] E. Garshick, A. Kelley, S. A. Cohen, A. Garrison, C. G. Tun, D. Gagnon, and R. Brown, "A prospective assessment of mortality in chronic spinal cord injury," *Spinal Cord*, vol. 43, no. 7, pp. 408–416, 2005. [Online]. Available: www.nature.com/sc

[9] G. G. Whiteneck, S. W. Charlifue, H. L. Frankel, M. H. Fraser, B. P. Gardner, K. A. Gerhart, K. R. Krishnan, R. R. Menter, I. Nuseibeh, D. J. Short, and J. R. Silver, "Mortality, morbidity, and psychosocial outcomes of persons spinal cord injured more than 20 years ago," Tech. Rep. 9, 1992.

[10] W. A. Bauman, A. M. Spungen, W. A. Bauman, W. A. Bauman, A. M. Spungen, R. H. Adkins, B. J. Kemp, R. H. Adkins, B. J. Kemp, and B. J. Kemp, "Metabolic and Endocrine Changes in Persons Aging with Spinal Cord Injury," *Assistive Technology*, vol. 11, no. 2, pp. 88–96, 1999. [Online]. Available: https://www.tandfonline.com/action/journalInformation?journalCode=uaty20

[11] S. W. Farrell, J. B. Kampert, H. W. Kohl, C. E. Barlow, C. A. Macera, R. S. Paffenbarger, L. W. Gibbons, and S. N. Blair, "Influences of cardiorespiratory fitness levels and other predictors on cardiovascular disease mortality in men," *Medicine and Science in Sports and Exercise*, vol. 30, no. 6, pp. 899–905, 1998.

[12] S. M. Grundy, J. I. Cleeman, S. R. Daniels, K. A. Donato, R. H. Eckel, B. A. Franklin, D. J. Gordon, R. M. Krauss, P. J. Savage, S. C. Smith, J. A. Spertus, and F. Costa, "Diagnosis and management of the metabolic syndrome: An American Heart Association/National Heart, Lung, and Blood Institute scientific statement," *Circulation*, vol. 112, no. 17, pp. 2735–2752, 2005.

[13] D. J. Green, G. O'Driscoll, M. J. Joyner, and N. T. Cable, "Exercise and cardiovascular risk reduction: Time to update the rationale for exercise?" *Journal of Applied Physiology*, vol. 105, no. 2, pp. 766–768, 2008.

[14] M. S. Nash, "Exercise as a health-promoting activity following spinal cord injury," *Journal of Neurologic Physical Therapy*, vol. 29, no. 2, pp. 87–106, 2005.

[15] D. T. Price, R. Davidoff, and G. J. Balady, "Comparison of cardiovascular adaptations to long-term arm and leg exercise in wheelchair athletes versus long-distance runners," *American Journal of Cardiology*, vol. 85, no. 8, pp. 996–1001, 2000.

[16] Y. Bhambhani, "Physiology of wheelchair racing in athletes with spinal cord injury," *Sports Medicine*, vol. 32, no. 1, pp. 23–51, 2002.

[17] S. R. Dearwater, R. E. Laporte, R. J. Robertson, G. Brenes, L. L. Adams, and D. Becker, "Activity in the spinal cord-injured patient: An epidemiologic analysis of metabolic parameters," *Medicine and Science in Sports and Exercise*, vol. 18, no. 5, pp. 541–544, 1986.

[18] W. M. Scelza, C. Z. Kalpakjian, E. D. Zemper, and D. G. Tate, "Perceived barriers to exercise in people with spinal cord injury," *American Journal of Physical Medicine and Rehabilitation*, vol. 84, no. 8, pp. 576–583, 2005.

[19] K. A. Curtis, G. A. Drysdale, R. D. Lanza, M. Kolber, R. S. Vitolo, and R. West, "Shoulder pain in wheelchair users with tetraplegia and paraplegia," *Archives of Physical Medicine and Rehabilitation*, vol. 80, no. 4, pp. 453–457, 1999.

[20] J. C. Bayley, T. P. Cochran, and C. B. Sledge, "The weight-bearing shoulder. The impingement syndrome in paraplegics," *Journal of Bone and Joint Surgery - Series A*, vol. 69, no. 5, pp. 676–678, 1987.

[21] W. E. Pentland and L. T. Twomey, "Upper limb function in persons with long term paraplegia and implications for independence: Part ii," *Paraplegia*, vol. 32, no. 4, pp. 219–224, 1994.

[22] W. P. Waring and F. M. Maynard, "Shoulder pain in acute traumatic quadriplegia," *Paraplegia*, vol. 29, no. 1, pp. 37–42, 1991.

[23] J. V. Subbarao, J. Klopfstein, and R. Turpin, "Prevalence and impact of wrist and shoulder pain in patients with spinal cord injury." *The journal of spinal cord medicine*, vol. 18, no. 1, pp. 9–13, 1995. [Online]. Available: https://www.tandfonline.com/action/journalInformation?journalCode=yscm20

[24] D. B. Barber and M. D. Gall, "Osteonecrosis: An overuse injury of the shoulder in paraplegia: Case report," *Paraplegia*, vol. 29, no. 6, pp. 423–426, 1991.

[25] S. W. Brose, M. L. Boninger, B. Fullerton, T. McCann, J. L. Collinger, B. G. Impink, and T. A. Dyson-Hudson, "Shoulder Ultrasound Abnormalities, Physical Examination Findings, and Pain in Manual Wheelchair Users With Spinal Cord Injury," *Archives of Physical Medicine and Rehabilitation*, vol. 89, no. 11, pp. 2086–2093, 2008.

[26] O. Jahanian, M. G. Van Straaten, B. M. Goodwin, R. J. Lennon, J. D. Barlow, N. S. Murthy, and M. M. Morrow, "Shoulder magnetic resonance imaging findings in manual wheelchair users with spinal cord injury," *Journal of Spinal Cord Medicine*, vol. 0, no. 0, pp. 1–11, 2020. [Online]. Available: https://doi.org/10.1080/10790268.2020.1834774

[27] T. K. Gill, E. M. Shanahan, D. Allison, D. Alcorn, and C. L. Hill, "Prevalence of abnormalities on shoulder MRI in symptomatic and asymptomatic older adults," *International Journal of Rheumatic Diseases*, vol. 17, no. 8, pp. 863–871, 2014.

[28] S. Lal, "Premature degenerative shoulder changes in spinal cord injury patients," *Spinal Cord*, vol. 36, no. 3, pp. 186–189, 1998.

[29] M. Dalyan, D. D. Cardenas, and B. Gerard, "Upper extremity pain after spinal cord injury," Tech. Rep. 3, 1999. [Online]. Available: http://www.stockton-press.co.uk/sc

[30] K. A. Curtis and D. A. Dillon, "Survey of wheelchair athletic injuries: Common patterns and prevention," Tech. Rep. 3, 1985.

[31] M. S. Ferrara and C. L. Peterson, "Injuries to athletes with disabilities: Identifying injury patterns," Tech. Rep. 2, 2000.

[32] M. S. Ferrara and R. W. Davis, "Injuries to elite wheelchair athletes," *Paraplegia*, vol. 28, no. 5, pp. 335–341, 1990.

[33] A. J. Dallmeijer, I. D. Zentgraaff, N. I. Zijp, and L. H. Van Der Woude, "Submaximal physical strain and peak performance in handcycling versus handrim wheelchair propulsion," *Spinal Cord*, vol. 42, no. 2, pp. 91–98, 2004.

[34] U. Arnet, *Handcycling : a biophysical analysis*, 2012. [Online]. Available: www.carbonbike.ch

[35] T. Abel, M. Kroner, V. S. Rojas, C. Peters, C. Klose, and P. Platen, "Energy expenditure in wheelchair racing and handbiking - a basis for prevention of cardiovascular diseases in those with disabilities," *European Journal of Preventive Cardiology*, vol. 10, no. 5, pp. 371–376, 2003.

[36] J. O. Totosy de Zepetnek, C. A. Pelletier, A. L. Hicks, and M. J. MacDonald, "Following the Physical Activity Guidelines for Adults With Spinal Cord Injury for 16 Weeks Does Not Improve Vascular Health: A Randomized Controlled Trial," *Archives of Physical Medicine and Rehabilitation*, vol. 96, no. 9, pp. 1566–1575, 2015.

[37] T. E. Nightingale, R. S. Metcalfe, N. B. Vollaard, and J. L. Bilzon, "Exercise Guidelines to Promote Cardiometabolic Health in Spinal Cord Injured Humans: Time to Raise the Intensity?" pp. 1693–1704, 2017.

[38] K. A. Ginis, A. L. Hicks, A. E. Latimer, D. E. Warburton, C. Bourne, D. S. Ditor, D. L. Goodwin, K. C. Hayes, N. McCartney, A. McIlraith, P. Pomerleau, K. Smith, J. A. Stone, and D. L. Wolfe, "The development of evidence-informed physical activity guidelines for adults with spinal cord injury," *Spinal Cord*, vol. 49, no. 11, pp. 1088–1096, 2011.

[39] L. Q. Su, J. M. Fu, S. L. Sun, G. G. Zhao, W. Cheng, C. C. Dou, and M. H. Quan, "Effects of HIIT and MICT on cardiovascular risk factors in adults with overweight and/or obesity: A meta-analysis," *PLoS ONE*, vol. 14, no. 1, pp. 1–21, 2019.

[40] O. W. Heyward, R. J. Vegter, S. De Groot, and L. H. Van Der Woude, "Shoulder complaints in wheelchair athletes: A systematic review," *PLoS ONE*, vol. 12, no. 11, pp. 1–20, 2017.

[41] C. R. Harnish, J. A. Daniels, and D. Caruso, "Training response to high-intensity interval training in a 42-year-old man with chronic spinal cord injury," *Journal of Spinal Cord Medicine*, vol. 40, no. 2, pp. 246–249, 2017.

[42] S. P. Hooker and C. L. Wells, "Effects of low- and moderate- intensity training in spinal cord-injured patients," *Medicine and Science in Sports and Exercise*, vol. 21, no. 1, pp. 18–22, 1989.

[43] X. Devillard, D. Rimaud, F. Roche, and P. Calmels, "Effects of training programs for spinal cord injury," *Annales de Readaptation et de Medecine Physique*, vol. 50, no. 6, pp. 490–498, 2007.

[44] T. A. Astorino and J. S. Thum, "Interval training elicits higher enjoyment versus moderate exercise in persons with spinal cord injury," *Journal of Spinal Cord Medicine*, vol. 41, no. 1, pp. 77–84, 2018.

[45] P. Schoenmakers, K. Reed, V. D. L. Woude, and F. J. Hettinga, "High intensity interval training in handcycling: The effects of a 7 week training intervention in able-bodied men," *Frontiers in Physiology*, vol. 7, no. DEC, pp. 1–9, 2016.

[46] C. Gauthier, R. Brosseau, A. L. Hicks, and D. H. Gagnon, "Feasibility, Safety, and Preliminary Effectiveness of a Home-Based Self-Managed High-Intensity Interval Training Program Offered to Long-Term Manual Wheelchair Users," *Rehabilitation Research and Practice*, vol. 2018, pp. 1–15, 2018. [Online]. Available: https://doi.org/10.1155/2018/8209360

[47] H. Faber, A. J. Van Soest, and D. A. Kistemaker, "Inverse dynamics of mechanical multibody systems: An improved algorithm that ensures consistency between kinematics and external forces," *PLoS ONE*, vol. 13, no. 9, pp. 1–16, 2018.

[48] R. Martinez, N. Assila, E. Goubault, and M. Begon, "Sex differences in upper limb musculoskeletal biomechanics during a lifting task," *Applied ergonomics*, vol. 86, no. March, p. 103106, 2020. [Online]. Available: https://doi.org/10.1016/j.apergo.2020.103106

[49] W. Wu, P. V. Lee, A. L. Bryant, M. Galea, and D. C. Ackland, "Subject-specific musculoskeletal modeling in the evaluation of shoulder muscle and joint function," *Journal of Biomechanics*, vol. 49, no. 15, pp. 3626–3634, 2016. [Online]. Available: http://dx.doi.org/10.1016/j.jbiomech.2016.09.025

[50] H. E. Veeger, L. A. Rozendaal, and F. C. Van der Helm, "Load on the shoulder in low intensity wheelchair propulsion," *Clinical Biomechanics*, vol. 17, no. 3, pp. 211–218, 2002.

[51] A. Inoue, E. Chosa, K. Goto, and N. Tajima, "Nonlinear stress analysis of the supraspinatus tendon using three-dimensional finite element analysis," *Knee Surgery, Sports Traumatology, Arthroscopy*, vol. 21, no. 5, pp. 1151–1157, 2013.

[52] D. H. Redepenning, P. M. Ludewig, and J. M. Looft, "Finite element analysis of the rotator cuff: A systematic review," pp. 73–85, jan 2020.

[53] M. G. Pandy and T. P. Andriacchi, *Muscle and joint function in human locomotion*, 2010, vol. 12.

[54] K. B. Shelburne, M. R. Torry, and M. G. Pandy, "Contributions of Muscles, Ligaments, and the Ground-Reaction Force to Tibiofemoral Joint Loading During Normal Gait," *Journal of Orthopaedic Research*, vol. 24, no. 10, pp. 1983–1990, 2006.

[55] H. E. J. Veeger, L. H. V. Van Der Woude, and R. H. Rozendal, "Load on the Upper Extremity in Manual Wheelchair Propulsion," Tech. Rep. 4, 1991.

[56] H. Abbasi Bafghi, A. De Haan, A. Horstman, and L. Van Der Woude, "Biophysical aspects of submaximal hand cycling," *International Journal of Sports Medicine*, vol. 29, no. 8, pp. 630–638, 2008.

[57] S. Van Drongelen, U. Arnet, L. H. Van Der Woude, and H. E. Veeger, "Propulsion effectiveness of synchronous handcycling," *Assistive Technology Research Series*, vol. 26, pp. 82–84, 2010.

[58] R. J. Vegter, B. S. Mason, B. Sporrel, B. Stone, L. H. van der Woude, and V. L. Goosey-Tolfrey, "Crank fore-aft position alters the distribution of work over the push and pull phase during synchronous recumbent handcycling of able-bodied participants," *PLoS ONE*, vol. 14, no. 8, pp. 1–14, 2019.

[59] C. Krämer, G. Schneider, H. Böhm, I. Klöpfer-Krämer, and V. Senner, "Effect of different handgrip angles on work distribution during hand cycling at submaximal power levels," *Ergonomics*, vol. 52, no. 10, pp. 1276–1286, 2010.

[60] G. Azizpour, A. Ousdad, G. Legnani, G. Incerti, M. Lancini, and P. Gaffurini, "Dynamic analysis of handcycling: Mathematical modelling and experimental tests," *Mechanisms and Machine Science*, vol. 47, pp. 33–40, 2017.

[61] G. Azizpour, M. Lancini, G. Incerti, P. Gaffurini, and G. Legnani, "An experimental method to estimate upper limbs inertial parameters during handcycling," *Journal of Applied Biomechanics*, vol. 34, no. 3, pp. 175–183, 2018.

[62] G. Legnani, G. Incerti, M. Lancini, and G. Azizpour, "An identification procedure for evaluating the dynamic parameters of the upper limbs during handcycling," *Proceedings of the ASME Design Engineering Technical Conference*, vol. 5A-2018, pp. 1–10, 2018.

[63] S. Van Drongelen, M. Schlüssel, U. Arnet, and D. Veeger, "The influence of simulated rotator cuff tears on the risk for impingement in handbike and handrim wheelchair propulsion," *Clinical Biomechanics*, vol. 28, no. 5, pp. 495–501, 2013.

[64] S. Van Drongelen, U. Arnet, L. van der Woude, and D. Veeger, "IS SYNCHRONOUS HANDCYCLING LESS STRAINING THAN HANDRIM WHEELCHAIR PROPULSION?" p. 55, 2004. [Online]. Available: http://eprints.uanl.mx/5481/1/1020149995.PDF

[65] E. Chiodi, "A biomechanical model of the upper limb applied to the handcycling," Ph.D. dissertation, 2016. [Online]. Available: http://repositorio.ual.es/bitstream/handle/10835/6429/10447_TFGEmanueleChiodi.pdf?sequence=1

[66] C. Kraaijenbrink, R. J. Vegter, A. H. Hensen, H. Wagner, and L. H. Van Der Woude, "Different cadences and resistances in submaximal synchronous handcycling in able-bodied men: Effects on efficiency and force application," *PLoS ONE*, vol. 12, no. 8, pp. 1–15, 2017.

[67] C. Kraaijenbrink, R. J. Vegter, A. H. Hensen, H. Wagner, and L. H. Van Der Woude, "Biomechanical and physiological differences between synchronous and asynchronous low intensity handcycling during practice-based learning in able-bodied men," *Journal of NeuroEngineering and Rehabilitation*, vol. 17, no. 1, pp. 1–13, 2020.

[68] S. Van Drongelen, J. van den Berg, U. Arnet, D. J. Veeger, and L. H. van der Woude, "Development and validity of an instrumented handbike: Initial results of propulsion kinetics," *Medical Engineering and Physics*, vol. 33, no. 9, pp. 1167–1173, 2011.

[69] L. Jakobsen and F. H. Ahlers, "Development of a wireless crank moment measurement-system for a handbike: Initial results of propulsion kinetics," Tech. Rep., 2016.

[70] B. S. Mason, B. Stone, M. B. Warner, and V. L. Goosey-Tolfrey, "Crank length alters kinematics and kinetics, yet not the economy of recumbent handcyclists at constant handgrip speeds," *Scandinavian Journal of Medicine and Science in Sports*, vol. 31, no. 2, pp. 388–397, feb 2021.

[71] O. J. Quittmann, J. Meskemper, T. Abel, K. Albracht, T. Foitschik, S. Rojas-Vega, and H. K. Strüder, "Kinematics and kinetics of handcycling propulsion at increasing workloads in able-bodied subjects," *Sports Engineering*, vol. 21, no. 4, pp. 283–294, 2018.

[72] O. J. Quittmann, T. Abel, K. Albracht, and H. K. Strüder, "Biomechanics of all-out handcycling exercise: kinetics, kinematics and muscular activity of a 15-s sprint test in able-bodied participants," *Sports Biomechanics*, 2020.

[73] U. Arnet, S. Van Drongelen, A. Scheel-Sailer, L. H. Van Der Woude, and D. H. Veeger, "Shoulder load during synchronous handcycling and handrim wheelchair propulsion in persons with paraplegia," *Journal of Rehabilitation Medicine*, vol. 44, no. 3, pp. 222–228, 2012.

[74] U. Arnet, S. van Drongelen, M. Schlüssel, V. Lay, L. H. van der Woude, and H. E. Veeger, "The effect of crank position and backrest inclination on shoulder load and mechanical efficiency during handcycling," *Scandinavian Journal of Medicine and Science in Sports*, vol. 24, no. 2, pp. 386–394, 2014.

[75] A. Faupin, P. Gorce, and C. Meyer, "Effects of type and mode of propulsion on hand-cycling biomechanics in nondisabled subjects," *Journal of Rehabilitation Research and Development*, vol. 48, no. 9, pp. 1049–1060, 2011.

[76] M. M. Rodgers, G. W. Gayle, S. F. Figoni, M. Kobayashi, J. Lieh, and R. M. Glaser, "Biomechanics of wheelchair propulsion during fatigue," *Archives of Physical Medicine and Rehabilitation*, vol. 75, no. 1, pp. 85–93, 1994.

[77] I. Rice, B. Impink, C. Niyonkuru, and M. Boninger, "Manual wheelchair stroke characteristics during an extended period of propulsion," *Spinal Cord*, vol. 47, no. 5, pp. 413–417, 2009.

[78] L. Qi, J. Wakeling, S. Grange, and M. Ferguson-pell, "Changes in surface electromyography signals and kinetics associated With Progression of Fatigue At Two Speeds During Wheelchair Propulsion," *Journal of Rehabilitation Research Development*, vol. 49, no. 1, pp. 23–34, 2012.

[79] O. J. Quittmann, T. Abel, K. Albracht, J. Meskemper, T. Foitschik, and H. K. Strüder, "Biomechanics of handcycling propulsion in a 30-min continuous load test at lactate threshold: Kinetics, kinematics, and muscular activity in able-bodied participants," *European Journal of Applied Physiology*, vol. 120, no. 6, pp. 1403–1415, jun 2020.

[80] D. J. Bregman, S. van Drongelen, and H. E. Veeger, "Is effective force application in handrim wheelchair propulsion also efficient?" *Clinical Biomechanics*, vol. 24, no. 1, pp. 13–19, 2009. [Online]. Available: http://dx.doi.org/10.1016/j.clinbiomech.2008.09.003

[81] D. J. Sanderson, "The influence of cadence and power output on the biomechanics of force application during steady-rate cycling in competitive and recreational cyclists," *Journal of Sports Sciences*, vol. 9, no. 2, pp. 191–203, 1991.

[82] S. Litzenberger, F. Mally, and A. Sabo, "Influence of different seating and crank positions on muscular activity in elite handcycling - A case study," *Procedia Engineering*, vol. 112, pp. 355–360, 2015. [Online]. Available: http://dx.doi.org/10.1016/j.proeng.2015.07.262

[83] R. Bini, P. Hume, J. Croft, and A. Kilding, "Pedal force effectiveness in Cycling: a review of constraints and training effects," *Journal of Science and Cycling*, vol. 2, no. 1, pp. 11–24, 2013. [Online]. Available: http://www.jsc-journal.com/ojs/index.php?journal=JSC&page=article&op=view&path[]=32

[84] A. C. of Sports Medicine et al., *ACSM's exercise testing and prescription*. Lippincott williams & wilkins, 2017.

[85] K. Mossberg, C. Willman, M. A. Topor, H. Crook, and S. Patak, "Comparison of asynchronous versus synchronous arm crank ergometry," pp. 569–574, 1999.

[86] K. D. Currie, J. B. Dubberley, R. S. McKelvie, and M. J. Macdonald, "Low-volume, high-intensity interval training in patients with CAD," *Medicine and Science in Sports and Exercise*, vol. 45, no. 8, pp. 1436–1442, 2013.

[87] J. P. Little, J. B. Gillen, M. E. Percival, A. Safdar, M. A. Tarnopolsky, Z. Punthakee, M. E. Jung, and M. J. Gibala, "Low-volume high-intensity interval training reduces hyperglycemia and increases muscle mitochondrial capacity in patients with type 2 diabetes," *Journal of Applied Physiology*, vol. 111, no. 6, pp. 1554–1560, 2011.

[88] K. A. Jacobs, P. Burns, J. Kressler, and M. S. Nash, "Heavy reliance on carbohydrate across a wide range of exercise intensities during voluntary arm ergometry in persons with paraplegia," *Journal of Spinal Cord Medicine*, vol. 36, no. 5, pp. 427–435, 2013.

[89] A. M. Cools, F. R. Johansson, D. Borms, and A. Maenhout, "Prevention of shoulder injuries in overhead athletes: A science-based approach," *Brazilian Journal of Physical Therapy*, vol. 19, no. 5, pp. 331–339, 2015.

[90] O. J. Quittmann, T. Abel, K. Albracht, and H. K. Strüder, "Reliability of muscular activation patterns and their alterations during incremental handcycling in able-bodied participants," *Sports Biomechanics*, 2019.

APPENDIX A

SUPPLEMENTAL DATA

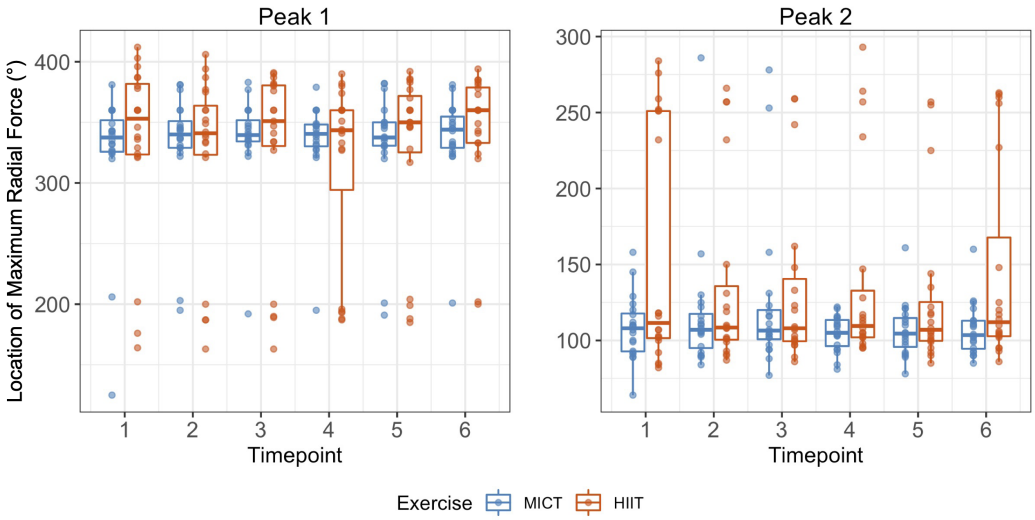

Figure 8: Location of radial force peaks across exercise protocols and at different timepoints. Extraneous points from altered propulsion styles can be seen around 200° (left plot) and 250° (right plot)

APPENDIX B

LOAD CELL COORDINATE TRANSFORMATIONS

Load cell data is filtered using a second-order low-pass Butterworth filter with a cutoff frequency of 10 Hz [90]. Force data is then downsampled from 2000 to 100 Hz to match the frequency of the motion capture data. To transform the raw x, y, and z load cell data onto the radial, tangential, and lateral directions, motion capture from the handcycle handle is used. Four markers were placed on the handcycle handle, labelled HandleTop, HandleBottom, CrankTop, and CrankBottom. An additional marker was placed on the load cell wire for redundancy in case of missing markers (Fig. 9).

For each frame during the trial, a radial unit vector $\hat{r} = \langle r_x, r_y \rangle$ and the crank angle, θ are created using the "CrankBottom" and "CrankTop" markers (Fig. 9). A perpendicular tangential unit vector $\hat{t}$ is then created using

$$\hat{t} = \langle r_y, -r_x \rangle \tag{B.1}$$

which is the equation for a clockwise perpendicular vector. The angle of the handle with respect to the horizontal, β, is then calculated using the "HandleTop" and "HandleBottom" markers.

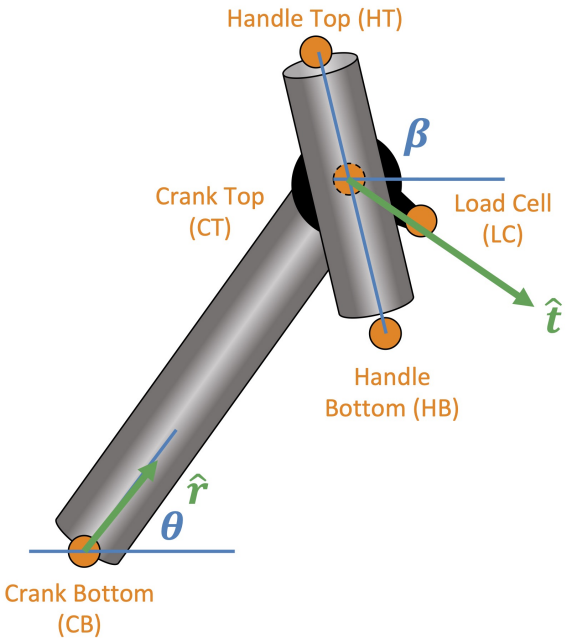

Figure 9: Load Cell Axis Transformation

The tangential force and tangential force vector will be created using two rotation matrices. The first rotation matrix converts the force components from the load cell coordinates to the handle coordinates. Because the load cell axes are at a 138° angle from the handle, the first rotation matrix, T_{LcH} is

$$T_{LcH} = \begin{bmatrix} cos(138°) & sin(138°) \\ -sin(138°) & cos(138°) \end{bmatrix} \tag{B.2}$$

Next, the force components need to be transformed from the handle axis, which changes for every timepoint depending on the handle angle, β, to the crank axis, which changes every time point depending on the crank angle, θ. Thus, the second transformation matrix, T_{HC} is dependant on both β and θ. To simplify this, we defined a new angle, γ, which is equal to $\theta - \beta$.

$$T_{HC} = \begin{bmatrix} cos(\gamma) & sin(\gamma) \\ -sin(\gamma) & cos(\gamma) \end{bmatrix} \tag{B.3}$$

Then, the forces are transformed using

$$\begin{bmatrix} F_t \\ -F_r \end{bmatrix} = T_{LcH} * T_{HC} * \begin{bmatrix} F_x \\ F_y \end{bmatrix} \tag{B.4}$$

We flip the sign of the radial force because, by our defined conventions, positive radial force is directed into the crank center.

F_{lat} is equivalent to F_z, and doesn't need to be transformed, as the load cell z-axis matches the global z-axis.

APPENDIX C

MISSING MARKER INTERPOLATION

Occasionally, one of the five motion capture markers on the handle is lost because it was knocked off or fell off during data collection. This occurs most commonly with the Handle Top and Handle Bottom markers because they are close to the hand on the handcycle handle. In this case, the fifth marker on the load cell wire (LC) is used with the remaining handle marker to interpolate the position of the missing marker during the trial (Fig. 10). For example, if Handle Top is missing for a time point, the Handle Bottom and LC markers are used to interpolate the position of Handle Top. Likewise, if Handle Bottom is missing during a time point, Handle Top and LC are used to interpolate the position of Handle Bottom.

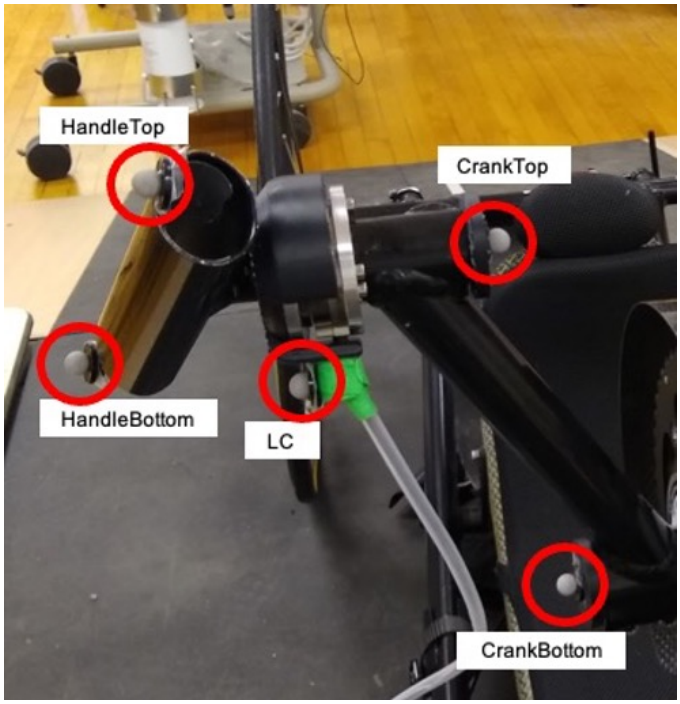

Figure 10: The 5 motion capture markers on the handcycle

To do this, a timepoint from the same exercise trial with all the markers is used as a baseline to determine the correct distances between the three handle markers (Fig 11). In Matlab, the length of segments A, B, and C is calculated from a frame of the reference trial.

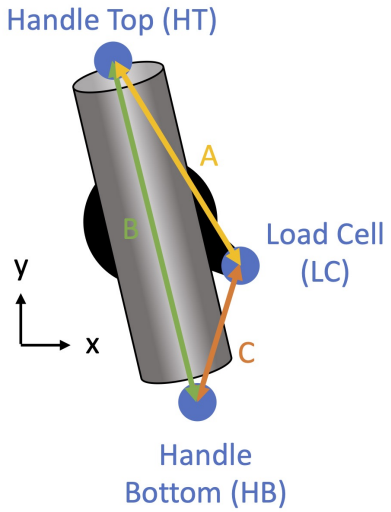

Figure 11: A, B, and C definitions from the reference frame in the timepoint with all three handle markers.

After A, B, and C are calculated, a system of equations is solved. Two circles are "drawn" that are centered around the two remaining markers, and the radii of the circles corresponds to the distance between that existing marker and the missing marker (Fig 12).

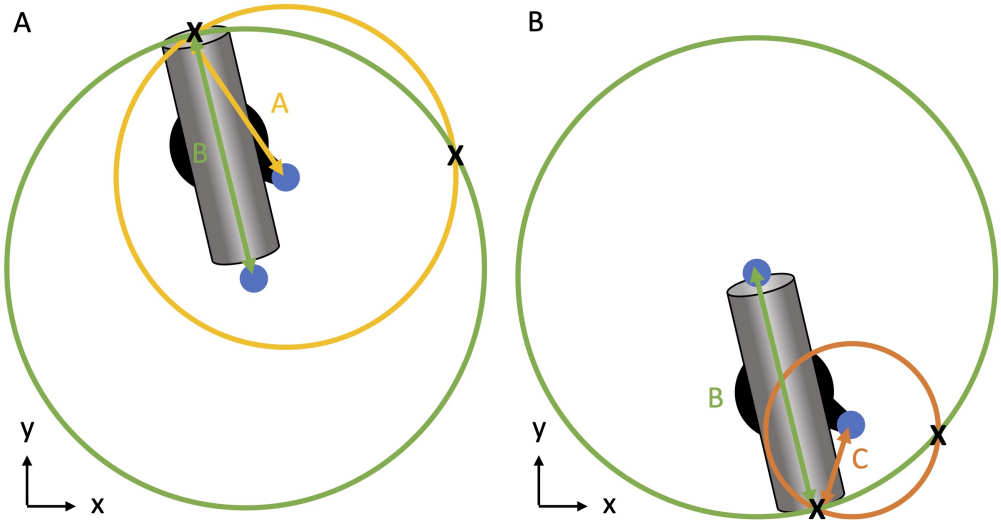

Figure 12: Circles drawn for A) Missing Handle Top marker, and B) missing Handle Bottom marker

If the Handle Top marker is missing, the system of equations is:

$$\begin{cases} (x - HB_x)^2 + (y - HB_y)^2 = B^2 \\ (x - LC_x)^2 + (y - LC_y)^2 = A^2 \end{cases} \tag{C.1}$$

Where x and y are the x and y-location of the Handle Top marker. Similarly, if the Handle Bottom marker is missing, the system of equations is:

$$\begin{cases} (x - HT_x)^2 + (y - HT_y)^2 = B^2 \\ (x - LC_x)^2 + (y - LC_y)^2 = C^2 \end{cases} \tag{C.2}$$

Where x and y are the x and y-location of the Handle Bottom marker. In both cases, solving the system of equations in MATLAB results in two possible x and y positions for the missing marker, because the circles intersect at two separate points, denoted by X's in Figure 12. If the Handle Top marker is missing, we choose the point with the smallest x-value. If the Handle Bottom marker is missing, we choose the point with the smallest y-value. This is done for each timepoint, and the missing marker location data is filled in and checked visually (Fig 13).

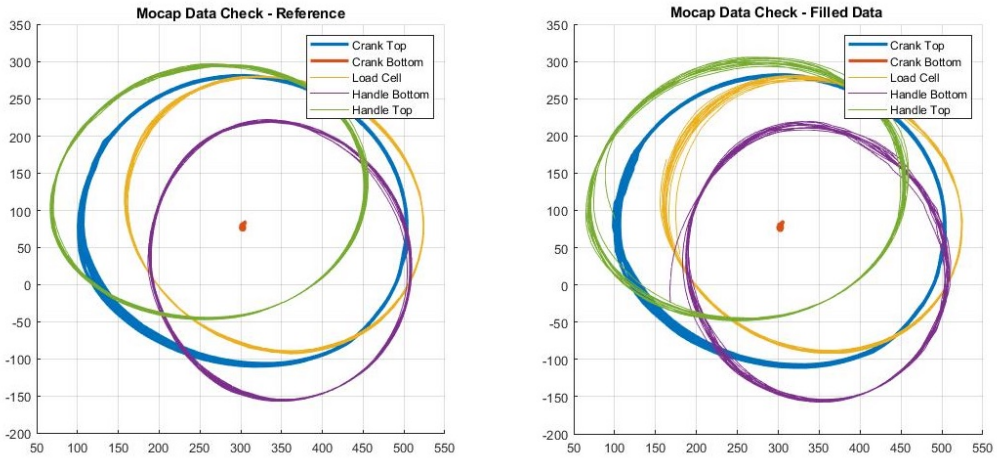

Figure 13: Reference location data (left) and filled data (right). In this example, the Handle Bottom marker, shown in purple, was missing from the trial and was filled in using the reference data and system of equations.